Analyzing Muffler Performance Using the Transfer Matrix Method

Author K.S. Andersen*
Dinex Emission Technology A/S
*Corresponding author: Fynsvej 39, DK-5500, Middelfart, Denmark, ksa@dinex.dk

Abstract: Exhaust noise must meet legislation targets, customer expectations and cost reduction which call for design optimization of the exhaust systems in the design phase. One solution is to use 3 dimensional linear pressure acoustics and calculate *the transfer matrix* of the muffler. The transfer matrix is the basis for calculating either the insertion loss or transmission loss of a muffler. The 3D simulations in Comsol of different muffler configurations are verified by measurements in a flow acoustic test rig using the two source method.

Keywords: Muffler, Transfer Matrix, Transmission Loss, Two Source Method.

1. Introduction

The noise from an exhaust system consists of three components: Pulsation noise and flow generated noise coming from the orifice of the muffler outlet and shell noise coming from the shell of the muffler.

Shell noise may be limited by using a stiffer or damped shell, while flow generated noise, such as turbulence and vortex shedding may be limited by minimizing geometrical discontinuities (edges, sharp bends etc.).

Minimizing pulsation noise, caused by the valves opening and closing inside the IC engine, is the focus of this paper and this is obtained by designing the internal parts of the muffler in such a way that the most critical part of the frequency spectrum is attenuated.

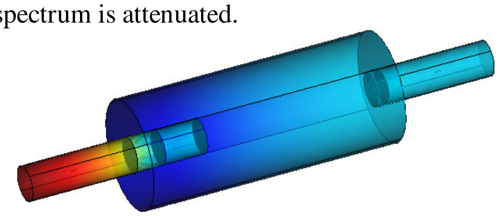

Figure 1. Comsol Multiphysics simulation of the sound pressure level at a frequency of 100 Hz.

2. Governing Equations

The governing equation of the sound field in a muffler is the linear time harmonic wave equation in three dimensions for acoustic pressure [1]

$$\nabla^2 p + k^2 p = 0 \qquad , k = \frac{\omega^2}{c^2} \tag{1}$$

ω is the angular frequency, k is the wave number, c is the speed of sound and p is the acoustic pressure.

The assumptions of linearity using a frequency model is valid for sound pressure levels up to 150 dB re 20 µPa, and for exhaust system lengths below 15 m, but nonlinearities may still occur at local constrictions such as perforated elements, due to high pulsating velocities [2]. In addition, a constant temperature through out the system is also assumed. Finally, the Mach number is set to zero, while the flow induced losses are implemented through the boundary conditions.

3. Methods

3.1 The CAE Tools

The available CAE tools for analyzing muffler performance includes 1D and 3D linear acoustic codes with and without mean flow, where the 3D may be either BEM or FEM based methods. Comsol Multiphysics offers a *3D linear acoustic* code where the most important effect of flow is included by altering the boundary conditions, while the mean flow is not included.

3.2 The Measurement Tools

The available measurement tools include sound pressure based insertion loss measurement by means of ISO 11820 in a reverberation room using real engines, transmission loss measurement using the three microphone method [3] and transfer matrix measurements by means of the 2-load or the 2-source method [4]. The *2-source method* was chosen as it offers the highest accuracy for comparison with the simulations.

4. Theory

4.1 The Plane Waves

The wave equation (1) for a single dimension, e.g. the x-direction in a duct, is

$$\frac{\partial^2 p}{\partial x^2}+k^2 p=0 \qquad ,k=\frac{\omega^2}{c^2} \tag{2}$$

The solution to the equation above may be written in sine and cosine functions or in exponential functions as

$$p(x)=p^+e^{-jkx}+p^-e^{jkx} \tag{3}$$

p(x) is a sum of two plane waves, one travelling in the positive x-direction with amplitude *p+* and the other in the negative x-direction with amplitude *p-*. The plane wave decomposition is shown in the figure below.

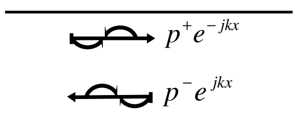

Figure 2. Plane wave decomposition in a duct.

By using Euler's equation for motion in a medium, the volume velocity is determined as

$$q(x)=\frac{S}{\rho_0 c}\left(p^+e^{-jkx}-p^-e^{jkx}\right), \tag{4}$$

where ρ_0 is the density and *S* is the duct area.

4.2 The Plane Waves in Mean Flow

The wave equation changes a little when mean flow is included

$$\frac{\partial^2 p}{\partial x^2}\left(1-M^2\right)+k^2 p-2jkM\frac{\partial p}{\partial x}=0, \tag{5}$$

where $M=u_0/c$ is the Mach number.

The solution is similar to equation (3), but the wave numbers are changed

$$p(x)=p^+e^{-jk_+x}+p^-e^{jk_-x} \tag{6}$$

$$k_+=\frac{k}{1+M} \quad ,k_-=\frac{k}{1-M}$$

The mean flow is stretching the waves in the same direction as the flow direction, while it is compressing the waves in the other direction.

4.3 The Transfer Matrix

When staying in the plane wave region for the inlet and outlet of the muffler, the muffler can be described by two port theory in form of either the scattering matrix, or the transfer matrix [4].

The sound pressure, p_i, and volume velocity, q_i, on the inlet side of a muffler may be fully transferred to the outlet side (p_o, q_o) by using the transfer matrix, ***T***, which consists of the four elements, T_{11}, T_{12}, T_{21}, T_{22},

$$\begin{pmatrix}\hat{p}_i\\ \hat{q}_i\end{pmatrix}=\begin{pmatrix}T_{11} & T_{12}\\ T_{21} & T_{22}\end{pmatrix}\begin{pmatrix}\hat{p}_o\\ \hat{q}_o\end{pmatrix} \tag{7}$$

The two-port theory assumes a linear and time invariant system, with continuity in sound pressure and volume velocity across transitions.

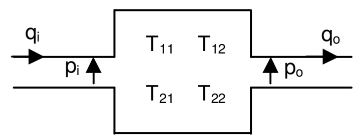

Figure 3. The basic transfer matrix parameters.

One advantage of using transfer matrices to describe a muffler is that you can connect multiple sub mufflers to one final muffler by just multiplying the matrices.

4.4 Transfer Matrix Extraction

A plane wave is applied at the inlet side and the muffler is terminated at both ends by an impedance match implemented by using the radiation condition. It is assumed that the sound field in the connecting ducts is only one dimensional, which is true for [1]:

$$f<\frac{1.84c}{\pi D} \tag{8}$$

D is the duct diameter and *f* is the frequency.

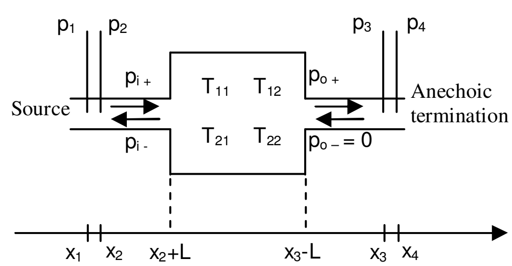

Figure 4. Parameters for extracting the transfer matrix.

When the equation system is solved, the acoustic pressure at two specific points on the inlet side (p_1, p_2) and on the outlet side (p_3, p_4) of the muffler are extracted for further calculations, where p_2, and p_3 has a numerical distance of L to the muffler.

$$
\begin{aligned}
p_1 &= p_{i+}\cdot e^{-jkx1} + p_{i-}\cdot e^{jkx1}\\
p_2 &= p_{i+}\cdot e^{-jkx2} + p_{i-}\cdot e^{jkx2}\\
p_3 &= p_{o+}\cdot e^{-jkx3} + p_{o-}\cdot e^{jkx3}\\
p_4 &= p_{o+}\cdot e^{-jkx4} + p_{o-}\cdot e^{jkx4}
\end{aligned} \tag{9}
$$

The left and right going pressure waves on the inlet side (p_{i-}, p_{i+}) and outlet side (p_{o-}, p_{o+}) of the muffler are.

$$
\begin{aligned}
p_{i+} &= \frac{j\left(p_1\cdot e^{jkx2} - p_2\cdot e^{jkx1}\right)}{2\sin k\left(x_1 - x_2\right)}\\
p_{o+} &= \frac{j\left(p_3\cdot e^{jkx4} - p_4\cdot e^{jkx3}\right)}{2\sin k\left(x_3 - x_4\right)}\\
p_{i-} &= \frac{j\left(p_2\cdot e^{-jkx1} - p_1\cdot e^{-jkx2}\right)}{2\sin k\left(x_1 - x_2\right)}\\
p_{o-} &= \frac{j\left(p_4\cdot e^{-jkx3} - p_3\cdot e^{-jkx4}\right)}{2\sin k\left(x_3 - x_4\right)}
\end{aligned} \tag{10}
$$

The sound pressures (p_i, p_o) and volume velocities (q_i, q_o) at the inlet and outlet plane of the muffler are (see figure 3).

$$
\begin{aligned}
p_i &= p_{i+}\cdot e^{-jk(x2+L)} + p_{i-}\cdot e^{jk(x2+L)}\\
q_i &= S\,\frac{p_{i+}\cdot e^{-jk(x2+L)} - p_{i-}\cdot e^{jk(x2+L)}}{\rho c}\\
p_o &= p_{o+}\cdot e^{-jk(x3-L)} + p_{o-}\cdot e^{jk(x3-L)}\\
q_o &= S\,\frac{p_{o+}\cdot e^{-jk(x3-L)} - p_{o-}\cdot e^{jk(x3-L)}}{\rho c}
\end{aligned} \tag{11}
$$

The transfer matrix is symmetric [1]

$$T_{11} = T_{22}\,, \tag{12}$$

and reciprocity requires the matrix determinant to be equal to one [1]

$$T_{11}T_{22} - T_{12}T_{21} = 1 \tag{13}$$

By using the two specific properties of the transfer matrix mentioned above, the four elements of the transfer matrix becomes

$$
\begin{aligned}
T_{11} &= \frac{p_o q_o + p_i q_i}{p_i q_o + p_o q_i} & T_{12} &= \frac{p_i^2 - p_o^2}{p_i q_o + p_o q_i}\\
T_{21} &= \frac{q_i^2 - q_o^2}{p_i q_o + p_o q_i} & T_{22} &= \frac{p_o q_o + p_i q_i}{p_i q_o + p_o q_i}
\end{aligned} \tag{14}
$$

4.5 Performance Evaluation

The acoustic performance of a muffler may be evaluated using either the transmission loss (*TL*) or the insertion loss (*IL*), while the flow performance is evaluated using the pressure loss (*PL*), also named the backpressure.

TL only depends on the muffler and not on the source (inlet and outlet length and impedance) and is considered the best parameter to use when comparing different methods and designs. *TL* in decibels is defined as the difference between the incident sound power and transmitted sound power, assuming a reflection free termination [3].

$$TL = 10\log\left(\frac{\left|p_{i+}\right|^2}{\left|p_{o+}\right|^2}\right) \tag{15}$$

TL may also be calculated using the transfer matrix elements [1].

$$TL = 10\log\left(\frac{1}{4}\left|T_{11} + T_{12}\frac{S}{\rho c} + T_{21}\frac{\rho c}{S} + T_{22}\right|^2\right) \tag{16}$$

IL depends on the source and is better to use when looking at individual practical solutions. *IL* is defined as the difference between the radiated sound power with a reference exhaust system (no muffler) and the radiated sound power with a muffler system [3].

PL, which is a gas dynamic parameter, depends only on the muffler and is defined as the difference between the static pressure before the muffler and the static pressure after the muffler.

TL will in this paper be used to evaluate the performance of the muffler.

5. Numerical Model

The boundary conditions inside the muffler are solid walls, coupling boundary conditions and perforated plates. The coupling boundary conditions are used to couple two connecting sub-domains, where sound will propagate unaffected, e.g. a duct connected to another duct. The perforated plates are implemented as a complex impedance, *Z*, where θ and χ are the real and imaginary part respectively [5].

$$\frac{Z}{\rho c} = \theta' + j\chi' \tag{18}$$

$$\theta' = \frac{1}{\sigma}\sqrt{\frac{8\mu k}{\rho c}}\left(1 + \frac{t}{d_h}\right) + \theta_f \tag{19}$$

$$\chi' = \frac{1}{\sigma}k\left(t + \delta_h\right) \tag{20}$$

The flow resistivity, θ_f, and the Comsol parameter for the diameter of the hole, d_h, are modified to account for flow induced losses. The modifications were done by comparing the real and imaginary part of the impedance to the model by T. Elnady [6]. The result were the below parameters, where σ is the porosity of the perforate and *d* is the actual diameter of the hole.

Table 1: Modified parts of the perforate impedance.

	Comsol	Dinex
Flow resistance (bias flow)	$\theta_f = 0$	$\theta_f = 1.57\dfrac{M}{\sigma}$
Flow resistance (grazing flow)	$\theta_f = 1$	$\theta_f = 0.5\dfrac{M}{\sigma}$
Hole diameter	$d_h = d$	$d_h = \left(81000k \cdot d^{1.5}\right)^{-1}$
End correction	$\delta_h = \dfrac{d_h}{4}$	$\delta_h = \dfrac{1}{4}d$

The medium in which the waves are traveling is either air or absorptive material described by Delany and Bazley [5]. The flow resistivity, R_f, of the absorptive material is estimated using the formula by Bies and Hansen [5], leaving only the apparent density σ_{ap} and the average fiber diameter, d_{av} to be determined.

$$R_f = 3.18 \cdot 10^{-9} \cdot \rho_{ap}^{1.53} \cdot d_{av}^{-2} \qquad (21)$$

6. Results

6.1 Experimental Setup

The experimental setup based, on the two source method, consists of a centrifugal fan feeding cold air into the muffler and 6 neodymium loudspeaker units for sufficient sound pressure level compared to flow generated noise.

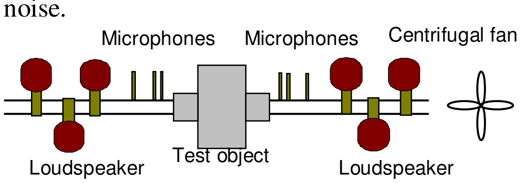

Figure 5. Layout of the flow acoustic test rig for experimental validation.

Six flushmounted ¼” B&K microphones for double frequency span are connected to the analyzer.

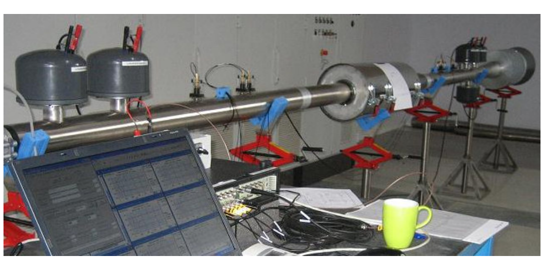

Figure 6. Picture of the flow acoustic test rig.

The signal from the stepped sine generator driving the loudspeakers, is used as reference for the microphone transfer functions, using 100 averages for enhancing the signal to noise ratio.

6.2 The Variable Standard Muffler

In order to verify the simulations, a variable standard muffler was constructed. Pictures of the basic three designs are shown below.

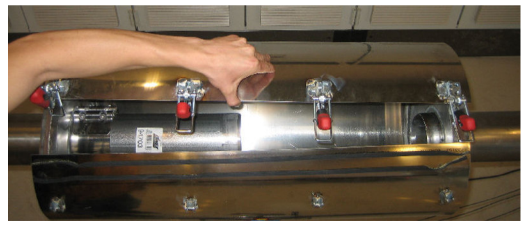

Figure 7. The reflective muffler.

Figure 8. The absorptive muffler.

Figure 9. The plug flow muffler.

6.2 The Reflective Muffler

The reflective muffler reflects the low frequency sound waves when the length of the *expansion chambers* or *quarter wave resonators* equals a multiple of a quarter of a wavelength.

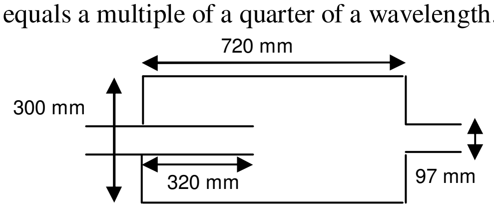

Figure 10. An expansion chamber with a resonator.

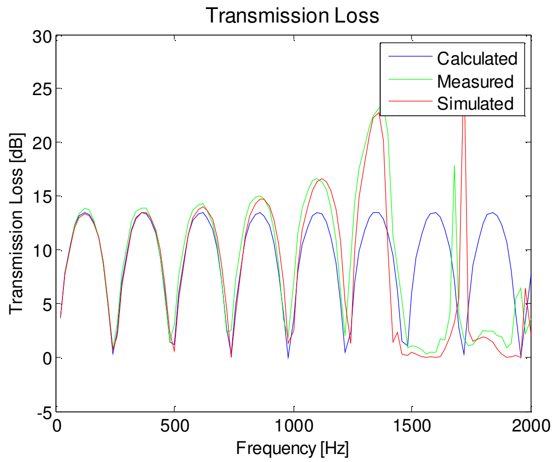

Figure 11. Transmission loss for a basic expansion chamber.

The measured and simulated transmission loss of the expansion chamber (figure 11) correlates well, besides a little offset in the peaks. This might be due to inaccuracies in different parameters (lengths, temperatures, densities etc.). A simple analytical calculation is also shown, and it does not capture the higher order modes. The first axisymmetric higher-order mode will start to propagate above 1400 Hz.

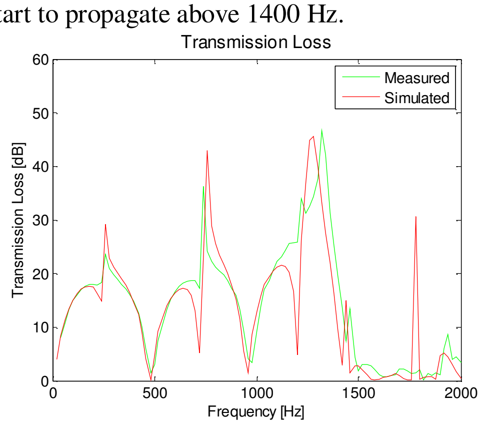

Figure 12. Transmission loss for an expansion chamber with a 320 mm quarter-wave resonator.

The measured and simulated transmission loss of an expansion chamber with a 320 mm quarter-wave resonator also exhibits good correlation even though the peaks are also shifted a little.

6.3 The Absorptive Muffler

The absorptive muffler works at mid and high frequencies by dissipating sound energy when the particle velocity of the sound waves is slowed during motion in the absorptive material. The effect of grazing flow in the perforate is limited compared to that of the absorptive material.

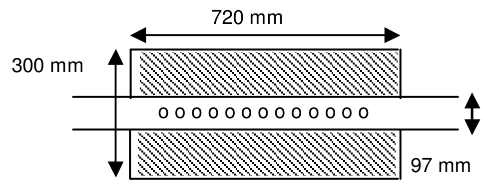

Figure 13. The absorptive muffler.

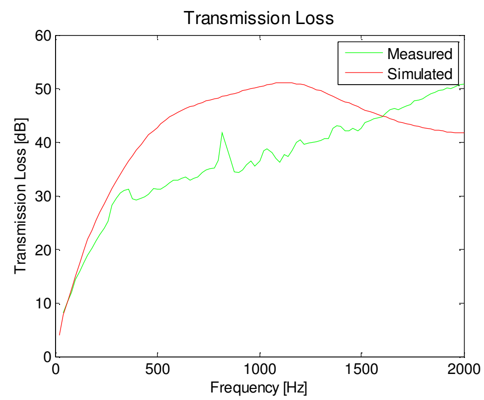

Figure 14. Transmission loss for a pure absorption muffler.

The effect of the absorptive material (R_f = 5000 Rayls/m) sets in above 100 Hz, and supplies a constant growing transmission loss (figure 14). The correlation is good until 350 Hz, above which the simulation at first overestimates, then underestimates the transmission loss. The Delany & Bazley model may be inaccurate when used in a sub domain as large as this. Additional tests with smaller sub domains could clarify this.

6.4 The Plug Flow Muffler

The plug flow muffler works at all frequencies by dissipating sound energy when vortices at the perforate interfere with the sound field. The flow in the perforate is now mainly bias flow in opposition to grazing flow.

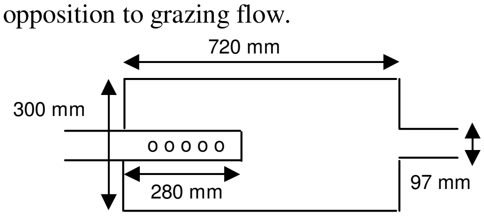

Figure 15. The plug flow muffler.

Figure 16. The perforated pipes used to verify the simulations. From left: Ø3 25.0%, Ø4 30.7%, Ø4 23.0%, Ø4 15.3%.

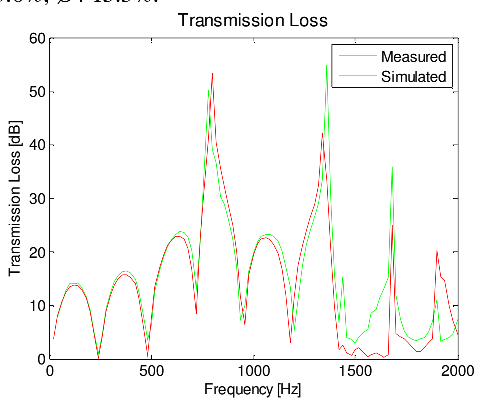

Figure 17. Transmission loss for a plug flow muffler. Ø3 mm holes with 25 % porosity at v = 0 m/s.

The simulation of the plug flow muffler (Ø3 mm holes and 25 % porosity) without flow, shown in figure 17, captures the resonator effect at 800 Hz due to the 80 mm extended inlet before the perforate section begins, though it underestimates the high frequency transmission loss.

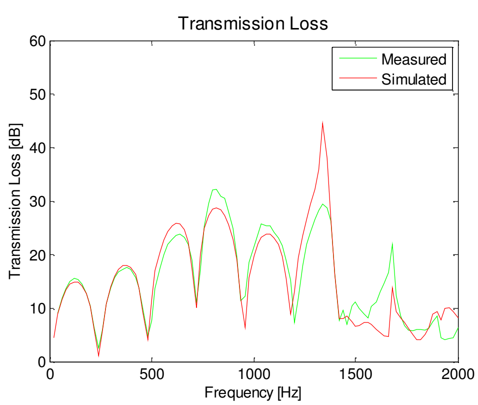

Figure 18. Transmission loss for a plug flow muffler. Ø3 mm holes with 25 % porosity at v = 30 m/s.

When a flow speed of v = 30 m/s is added (figure 18), the simulation captures the smoothing of the peaks and dips, except for the peak at 1350 Hz.

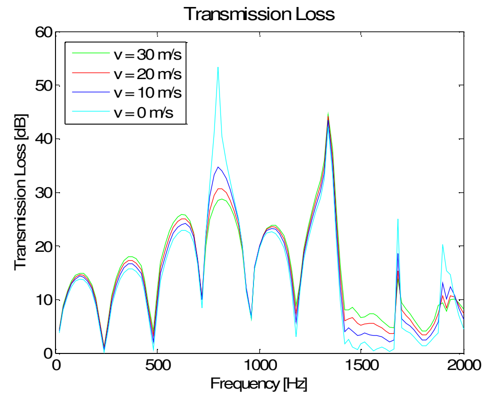

Figure 19. Simulated transmission loss for a plug flow muffler. Ø3 mm holes with 25 % porosity at different flow speeds.

Increasing flow velocities increases the smoothing of the peaks and dips which is seen in figure 19.

The flow in an automotive exhaust system is pulsating (in opposition to a constant flow), hence the effect of the perforate increase in real applications.

The figure below shows that decreasing the porosity has the same effect as increasing the velocity, since they are both included as a real part of the impedance in the boundary condition for the perforate. Additional simulations and measurements have shown that the diameter of the holes in the perforate may be varied between 3 mm and 12 mm without any significant influence.

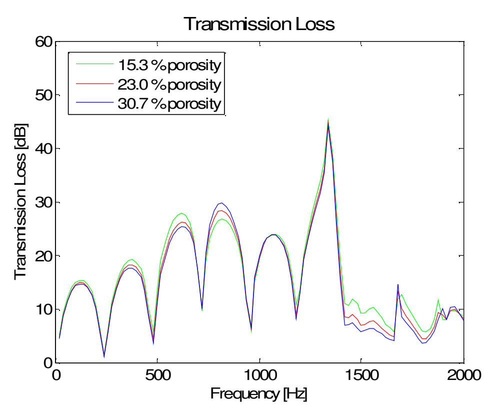

Figure 20. Simulated transmission loss spectrum for a plug flow muffler Ø4 mm holes with different porosities at v = 30 m/s.

6.5 Simulation setup

Setting up a model takes about 20 minutes from importing the CAD model to hitting the solve button, while the solution time is 10 minutes when taking 100 frequency steps and using 5 elements pr. wavelength and solving the system using the PARDISO solver on a normal desktop pc.

8. Conclusions

This paper shows how the transfer matrix may be extracted using the complex wave amplitudes at two specific points on the inlet side and outlet side, while running only a single simulation at multiple frequencies.

This method makes it possible to calculate the insertion loss in opposition to the direct calculation of the transmission loss based on an integration of the pressure across the inlet and outlet of the muffler [5].

The simulation results of the reflective muffler and the plug flow muffler with perforate correlate well with the measurements, but work needs to be done in the field of absorption in order to trust the simulations of the absorptive muffler. The model settings could be updated using the measurements.

No frequency limitations, short setup time, and easy redesign are among the advantages of using 3D pressure acoustic simulation while the down sides reads relatively long simulation time compared to 1D acoustic codes and no "easy" pressure loss simulation.

Still this approach is faster than using 1D gas dynamic codes.

8. Perspectives

The confidence achieved in the simulation procedure makes it possible for Dinex to mainly use simulations in the early design phase.

Future work will involve simulation of pressure loss and mean flow distribution by perhaps using impedance implementation of the perforated elements.

The transfer matrices obtained will be of real value, when the source impedance of a real engine can be used together with the transfer matrix to calculate the insertion loss, and later on compared to direct measurements according to ISO 11820.

Finally the simulations will be used to optimize production parameters such as minimal material consumption, simple construction, simple production and small.

9. References

1. A. D. Pierce, *Acoustics – An Introduction to Its Physical Principles and Applications*, page 17, 317, 351, 353. Acoustical Society of America, (1989)
2. H. Bodén, M. Åbom, Modelling of Fluid Machines as Sources of Sound in Duct and Pipe Systems, *Acta acustica*, **3**, p. 549-560 (1995)
3. M. L. Munjal, *Acoustics of Ducts and Mufflers*, page 21, 55-59, 201-205. John Wiley & Sons, Inc., (1987)
4. M. Åbom, Measurement of the Scattering-matrix of Acoustical Two-ports, *Mechanical Systems and Signal Processing*, **5(2)**, 89-104 (1991)
5. COMSOL 3.4, *Acoustic Module Model Library*, 74-89, 154-170. COMSOL AB (2007)
6. T. Elnady, *Modelling and characterization of Perforates in Lined Ducts and Mufflers*, doctoral dissertation. Dept. Aeronautical and Vehicle Eng., Royal Institute of Technology, Stockholm (2004)

10. Acknowledgements

Mats Åbom and Hans Bodén at KTH for practical help during design of the flow rig.

Tamer Elnady at Ain Shams University for help with the experimental data analysis.

Christian Svendsen at Danfoss Compressors GmbH for help with the automation of the measurements.

Mads Nygaard, Henrik Breiner Jensen, Mads Juul Jacobsen and Carsten Thiel at Dinex Emission Technology A/S for help with the construction of the flow rig.

And finally Comsol support for continuously helping with simulation problems.